Oblique wave interaction with reflective structures by a high-order velocity potential Boussinesq-type model

E. Jamois[(1,2)], D.R. Fuhrman[(3)], H.B. Bingham[(3)], B. Molin[(1)], F. Remy[(1)]

(1) Ecole Généraliste d'Ingénieurs de Marseille[1], 13 451 Marseille cedex 20, France
(2) Saipem SA, 78 884 Saint-Quentin Yvelines cedex, France
(3) Department of Mechanical Engineering, Technical University of Denmark, DK-2800 Kgs. Lyngby, Denmark

Abstract. This paper focuses on a high-order velocity potential Boussinesq-type approach to compute highly-nonlinear wave interaction with reflective coastal structures. This method proposed by Jamois *et al.* (2005) has already shown the capability to take the large wave amplification phenomenon occurring in front of reflective structures presented in Molin *et al.* (2005) into account. This phenomenon is due to third-order interactions between the incoming and reflected wave fields on the weather side of the structure. The numerical model presented here has been already validated on deep water experiments conducted on a vertical plate model subjected to waves of normal incidence. We report here a new extension of the model to oblique wave generation and our first results on cases involving run-up on a vertical plate subjected to oblique waves. It is observed that run-up effects decrease as the angle of the incoming waves increases.

1 Boussinesq-type approach

The Boussinesq method used here is based on the equations derived in Madsen *et al.* (2003). These equations retain only up to third order derivatives with respect to velocities and are expressed in terms of velocity potential instead of the commonly used horizontal velocities variables. The model is shown to accurately propagate dispersive nonlinear waves up to dimensionless water depths of $kh \approx 10$ and the linear internal wave kinematics are accurate up to $kh \approx 3.5$. Consider the irrotational flow of an incompressible inviscid fluid with a free surface. A cartesian coordinate system is adopted, with the x-axis and y-axis located on the still-water plane and with the z-axis pointing vertically upwards. The fluid domain is bounded by the sea bed at $z = -h(x, y)$ and the free surface at $z = \eta(x, y, t)$.
Following Zakharov (1968), the free surface boundary conditions are written in terms of velocity potential $\tilde{\phi} = \phi(x, y, \eta, t)$ and vertical velocity $\tilde{w} = (\phi_z)_{z=\eta}$ defined at the free surface :

$$\eta_t + \nabla\eta \cdot \nabla\tilde{\phi} - \tilde{w}(1 + \nabla\eta \cdot \nabla\eta) = 0 \tag{1}$$

$$\tilde{\phi}_t + g\eta + \frac{1}{2}(\nabla\tilde{\phi})^2 - \frac{1}{2}\tilde{w}^2(1 + \nabla\eta \cdot \nabla\eta) = 0 \tag{2}$$

where $\nabla = \{\partial/\partial x, \partial/\partial y\}$ is the horizontal gradient operator and $g = 9.81\ m/s^2$ the gravitational acceleration. Integrating η and $\tilde{\phi}$ in time requires a means of computing the associated $\tilde{w}$, satisfying the Laplace equation in the interior fluid domain and the kinematic bottom boundary condition given below :

$$w + \nabla h \cdot \nabla\phi = 0, \qquad z = -h(x, y) \tag{3}$$

The vertical distributions of the variables in the fluid are approximated by the following expressions :

$$\phi(x, y, z, t) \approx (1 - \alpha_2\nabla^2)\hat{\phi^*} + ((z - \hat{z}) - \beta_3\nabla^2)\hat{w^*} \tag{4}$$

$$w(x, y, z, t) \approx (1 - \alpha_2\nabla^2)\hat{w^*} - ((z - \hat{z})\nabla^2 - \beta_3\nabla^4)\hat{\phi^*} \tag{5}$$

[1]Contact : jamois@esim.fr

where $\alpha_2 \equiv \frac{1}{2}(z-\hat{z})^2 - \frac{1}{10}\hat{z}^2$ and $\beta_3 \equiv \frac{1}{6}(z-\hat{z})^3 - \frac{1}{10}\hat{z}^2(z-\hat{z})$. In (4-5) the utility variables $\hat{\phi^*}$ and $\hat{w^*}$ allow the introduction of Padé operators in the approximations resulting in far more accurate equations. Optimal kinematics properties are obtained through expansions done about the level $z = \hat{z} = -\frac{h}{2}$ in the water column. The kinematic bottom boundary condition relates $\hat{\phi^*}$ and $\hat{w^*}$ to each other and the expansion (4) relates the velocity potentials defined at the free surface and expressed at $z = \hat{z}$. The resulting 2 x 2 linear system to be solved is written: $\mathbf{Ax} = \mathbf{b}$, where $x = \{\hat{\phi^*}, \hat{w^*}\}$ and $b = \{\tilde{\phi}, 0\}$. Thus the vertical velocity at the free surface $\tilde{w}$ can be computed from (5), which closes the problem and allows the marching in time in the model. The numerical method used here is based on the numerical recipes proposed in Fuhrman and Bingham (2004) and is fully described in Jamois *et al.* (2005). To include fixed rectangular box-shaped structures into the fluid domain, a staggered obstacle technique on a uniform rectangular grid is used. Thus, the structure is lying half way between grid points. For exterior corner points the boundary conditions for mixed derivatives are imposed following Bingham *et al* (2005). The filtering used throughout this work has been analysed in Jamois *et al.* (2005). A local filtering is used once per time step around structural exterior corners and one general smoothing over all the domain is used once per wave period in case of highly-nonlinear waves (*e.g.* when some breaking located on wave crests was observed during experiments).

2 Oblique wavemaker

In order to generate oblique waves efficiently, a numerical set-up composed of six zones is used. Two generation zones are located at one of the side-walls and at the entrance of the domain. Two sponge layers are situated at one of the side-walls and at the end of the domain to absorb outgoing waves. Two relaxation zones placed in front of generation zones allow the damping of backward reflected wave fields due to the structure. Input wave conditions are computed using the theoretical stream function solution given by Fenton (1988). As an initial condition, it is imposed on one part of the domain. To prevent the numerical solution from disturbing diffraction processes, the stream function solution at the side-wall is imposed gradually over the domain by using a ramping function advancing in time at the group velocity of the incoming wave field. The size of the lateral sponge layer depends on the angle of propagation of the incoming wave field and is shown to be related to the normal wavenumber component, $l_{sponge} \approx 2(\frac{2\pi}{k_x})$ for waves propagating along the y-direction. For angles less than 10°, the numerical cost of a sponge layer is too expensive. The alternative is to enlarge sufficiently the fluid domain. Thus, the structure can be placed away from any disturbing reflection from the side wall which will be finally absorbed by the sponge layer located at the end of the domain. Results in both

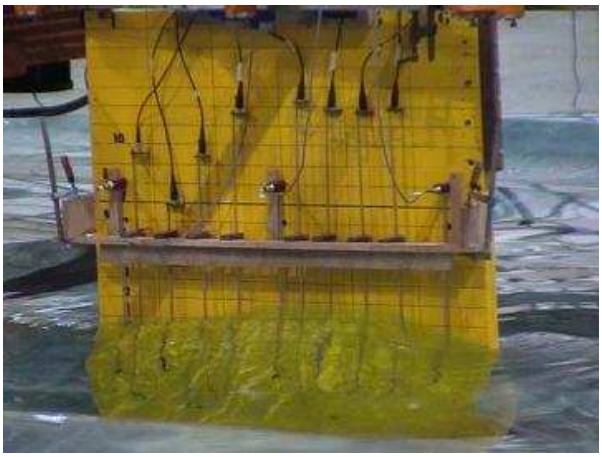

Figure 1: Experimental set up on the plate.

configurations are given in the next section. The main restriction of this numerical set-up is the size of the lateral damping zone. Fortunately, the use of equations expressed in terms of velocity potential, allow the model to handle very large domains due to a decrease of the computational effort (by a factor of two) compared to a classical velocity formulation.

3 Results

We present here numerical investigations on the sensitivity of the run-up in front of a vertical plate model to the angle of incidence of the incoming wave field. The test cases are based on a preliminary experimental campaign that has been done in the BGO-FIRST offshore wave tank in La Seyne sur Mer (France). The experiments were conducted on a vertical rigid plate 1.2 m long, 2 m high and 5 cm wide located in the middle of the basin, which is 16 m wide and about 30 m long. Figure 1 presents the experimental set up on the plate. The depth was $h = 1.2$ m. The plate was submitted to regular waves of varying periods and steepnesses and located at about 14 m from the wavemakers. We consider the wave period $T = 0.8$ s, which corresponds for linear waves to a wavelength $L = 1$ m, and the incoming wave steepness $H/L \approx 0.06$. Four different wave incidences were carried out for this particular case: 0°, 5°, 10° and 20°. During the experiments, instead of generating oblique waves, the plate model was rotated up to the corresponding angles and normal waves were generated. Unfortunately, due to a problem with the control of the wavemaker motion, the experimental results of this campaign are not reliable enough to be compared to numerical results and consequently only numerical solutions are shown here. Tests on a similar experimental set-up will be soon reconducted and comparisons with numerical results will be presented at the workshop. In the numerical simulations, the depth has

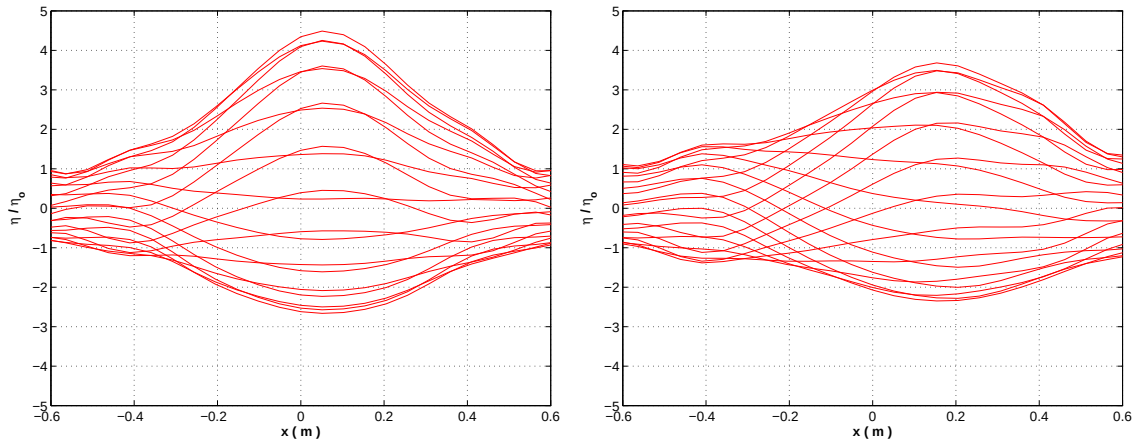

Figure 2: Computed free surface envelopes along the plate on the weather side at a stationary state for $T = 0.8$ s, $H/L \approx 0.06$, 1° (left) and 5° (right).

been reduced to $h = 0.65$ m, leading to $kh \approx 4$. The discretization used is $\Delta y = \Delta x = L/20$ m and $\Delta t = T/20$ s. When using a lateral sponge layer, the width of the useful numerical basin has been reduced to 12 m as the lateral boundary conditions correspond to radiation conditions. In case of small angles the width of the domain has been enlarged up to 17 m in the most critical case, *i.e.* 5° here. The plate dimensions are 1.2 x 0.10 m due to the stencil used which is limiting the width of any structure to $2\Delta y$. All simulations were run in order to reach stationary states. Firstly, to demonstrate the high sensitivity of the run-up to the angle of wave incidence, Figure 2 shows the computed free surface envelopes along the GBS for an incidence of 1°. It can be seen that under these conditions the maximum of wave elevation in front of the structure is not located in the middle of the plate as expected under normal incidence due to the symmetry of the problem. Figures 2 and 3 give the results obtained for incidences of 5°, 10° and 20°.

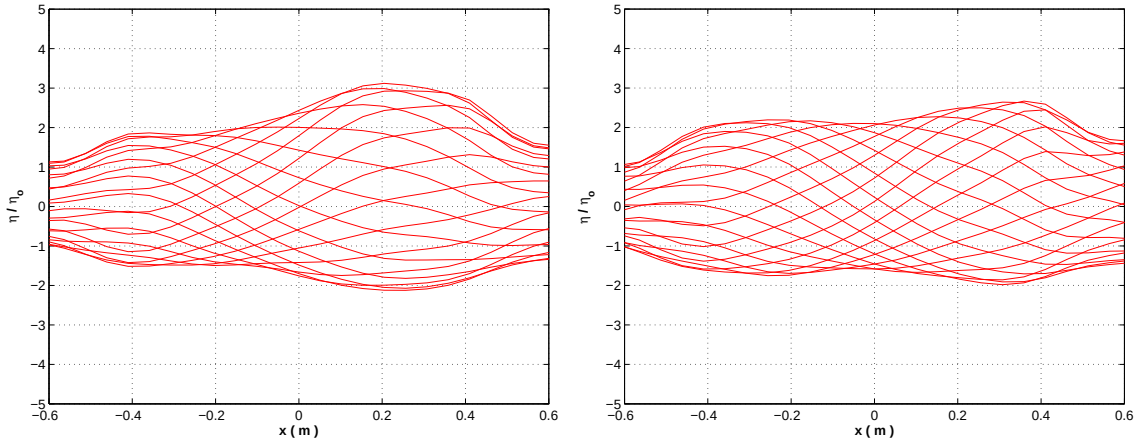

Figure 3: Computed free surface envelopes along the plate on the weather side at a stationary state for $T = 0.8$ s, $H/L \approx 0.06$, 10° (left) and 20° (right).

For small angles, large amplifications are observed confirming that in case of important reflected wave fields, strong nonlinear interactions related to third order effects take place on the weather side of the structure. These create some focus points on the structure, where an amplification factor of about 4.5 in the wave height is predicted in the most critical case, *i.e.* 1° here. This results in a nearly standing wave of steepness $H/L > 0.2$ and underlines the capability of the formulation to model extremely nonlinear waves. In case of an oblique incident wave field, the maximum of the free surface elevation shifts gradually to one side of the plate when the angle of attack increases. For angles of propagation greater than 20°, the large run-ups related to third order interactions disappear leading to a maximum factor of amplification of 2.65 in front of plate, which is close to a linear case result. The reflected and incoming wave fields do not interact enough to create any nonlinear focusing on the plate.

References

Bingham H.B., Fuhrman D.R., Jamois E. & Kimmoun O. 2004 Nonlinear wave interaction with bottom-mounted structures by a high-order Boussinesq method, *Proc. 19th Int. Workshop on Water Waves and Floating Bodies*, Cortona, Italy.

Fenton J.D. 1988 The numerical solution of steady water waves problems, *Computers and Geosciences*, **14**, 357–368.

Fuhrman D.R. & Bingham H.B. 2004 Numerical solutions of fully non-linear and highly dispersive Boussinesq equations in two horizontal dimensions, *Int. J. Numer. Meth. Fluids*,**44**, 231–255.

Jamois E., Kimmoun O., Molin B. & Stassen Y. 2004 Nonlinear interactions and wave run-up near a gravity base structure, *Proc. ICCE Conf.*, Lisbonne.

Jamois E., Fuhrman D.R. & Bingham H.B. 2005 Wave-structure interactions and nonlinear wave processes on the weather side of reflective structures, in preparation.

Madsen P.A., Bingham H.B. & Schaffer H.A. 2003 Boussinesq-type formulations for fully nonlinear and extremely dispersive water waves, *Proc. R. Soc. Lond. A*, **459**, 1074–1104.

Molin B., Remy F., Kimmoun O. & Jamois E. 2005 The role of tertiary wave interactions in wave-body problems, *J. Fluid Mech.*, in press.

Zakharov V.E. 1968 Stability of periodic waves of finite amplitude on the surface of a deep fluid, *J. Appl. Mech. Tech. Phys.*, **9**, 190–194.